Available online at www.pelagiaresearchlibrary.com

Pelagia Research Library

Der Chemica Sinica, 2012, 3(3):589-601

Pelagia Research Library
ISSN: 0976-8505
CODEN (USA) CSHIA5

Comparative Study of Physical and Thermal Properties of Chitosan-Silica Hybrid Coatings Prepared by Sol-Gel Method

Prerna Dhawade* and Ramanand Jagtap

Department of Polymer and Surface Engineering, Institute of Chemical Technology, Matunga, Mumbai, India

---

ABSTRACT

Organic-inorganic hybrid coatings have been prepared by sol-gel method of chitosan with different silanes. Silane precursors used in these coatings are glycidoxypropyltrimethoxysilane (GPTMS), Tetramethoxysilane (TEOS) and vinytrimethoxysilane (VTMS). The hybrid coatings have been evaluated by AT-FTIR and ^{13}C-NMR analysis for their structural features, which confirms the formation of siloxane-polymer network and provide the evidence of different silanes used. An XRD result presents crystalline structure of chitosan-silica hybrid coatings. It illustrate that the aggregation of silica in hybrid coatings differs with the silane used in hybrid coatings. The structural modification occurring due to different silane precursors is responsible for more thermal stability of hybrid coatings than pristine chitosan. Differential scanning calorimetry (DSC) presents the glass transition temperature of hybrid coatings. The water wettability of hybrid coatings is measured by contact angle analysis. The contact angle values of hybrid coatings with respect to polar and non-polar solvent assures the surface reorganization during contact angle measurements. Surface energy explains the behavior of liquids on the hybrid coatings. The surface morphology and roughness of hybrid coatings are well explained by SEM and AFM studies. The wettability and surface morphology of hybrid coatings differ by the use of different silanes used in the hybrid coatings.

Keywords: Sol-gel, Chitosan-silica hybrid coatings, Wettability, Thermal properties, SEM, AFM.

INTRODUCTION

Research and industries interest are on the rise in the advanced materials developed by combination of macromolecules with inorganic species to form organic-inorganic hybrid materials [1]. Sol-gel technology offers simple and convenient method for the preparation of organic–inorganic composite materials based on hybridization on molecular level [2]. The preparation of these hybrid materials are divided into two methods. One is the formation of composite materials on which organic material is supported. The other one is hybrid material formed by sol-gel method. This organic-inorganic hybrid material is formed by the hybridization of organic constituent with the inorganic constituent. Silica has been shown to be a good candidate as supporting material because of its large surface area and excellent mechanical resistance [3,4]. These organic-inorganic hybrid materials possess catalytic, optical, thermal and mechanical properties due to physical and chemical interactions between organic and inorganic constituents [5]. Thus, they are widely applicable in diverse fields [6-10]. Sol-gel method develops xerogel coatings which are economical and environmental friendly [11].

Sol-gel method has been widely used for the preparation of organic-inorganic hybrid materials. The inorganic network is obtained from metal-alkoxysilanes via hydrolysis-condensation mechanism. The chemical reactions can be described schematically as follows:

Si OR + H2O Si OH + ROH (1)

Si OR + HO Si Si O Si + ROH (2)

Si OH + HO Si Si O Si + H2O (3)

The silanol group (Si–OH) produced by the hydrolysis reaction, (1), is converted into siloxane (Si–O–Si) crosslinks by either reaction (2) or reaction (3).

Sol-gel process is employed to form biopolymer-silica hybrid materials which have recently drawn attention due to their potential properties, compatibility with living matters and they also relate to biomimmetic processes [12-16]. These hybrid materials are prepared by a controlled sequence of hydrolyses and condensations starting from an alkoxysilane like tetraethyl silicate in alcohols and other polar solvents leads to a solution or colloidal suspension of siloxane polymers (sol) [17]. At this stage, or at the beginning of the process, it is possible to incorporate a soluble organic polymer in the sol. These organic-inorganic hybrid materials exhibit unique mechanical properties such as high ductility, low elastic modulus and high mechanical strength [18]. Literature reveals the formation of different polyssacharide silica hybrid coatings such as cellulose/silica [19], chitosan/silica [1, 20-22], chitosan/titania [23], and cellulose/titania [24]. These biopolymer-silica hybrid materials find application in various fields such as bone substitutents, cements for bone repair and construction, enzyme and cell immobilization, catalysis and sensors [25-28]. These organic-inorganic hybrid materials prepared by the combination of organic-inorganic hybrids are used in the form of films for membranes or coatings or as precursors for the preparation of porous materials [29].

Chitosan is a biodegradable polymer obtained by alkaline deacetylation of chitin. It is a linear copolymer of 2-acetamido-2-deoxy-D-glucopyranose and 2-amino-2-deoxy-D-glucopyranose joined by β (1,4) glycosidic bonds. Chitosan is nontoxic, biodegradable, biocompatible polymer having inherent film forming and heat resistant property [30]. Chemical modification of chitosan becomes feasible due to presence of amino and hydroxyl groups in it, which makes it attractive for the preparation of hybrid materials [20-22, 30]. Chitosan has broad spectrum antimicrobial activity against fungi, algae and bacteria [31-33]. Antimicrobial activity also enhances its application in various fields such as biomedical [34,35,36,37], food [38], textile [39], waste water treatment [40], adsorption [41], interior finishing coatings for formaldehyde adsorption [42], dyes [43] and complex formation [44].

Chitosan-inorganic materials have recently attracted much attention due to its potential in scientific and technical application which provides combination properties of both organic and inorganic species. Chitosan silica hybrid materials with different characteristics are applied in various fields according to their requirement [1, 45, 46].

In this paper we have prepared chitosan/silica hybrid materials using chitosan and different silanes by sol-gel method at ambient temperature. The aim of this study was to make use of the expected tendency of this biopolymer for association with silicate hydrosols in order to modify the characteristics of the products. We present a systematic study of physical and chemical properties of these hybrid materials. The chemical structures of chitosan/silica hybrid materials differ by the use of different silanes which are used for the preparation of these hybrid materials. These differences in their chemical structures are explained by AT-FTIR and ^{13}C-NMR analyses. The effect of different silanes on thermal stability, wettability and surface roughness of hybrid materials are deeply investigated by various analyses.

MATERIALS AND METHODS

Chitosan-siloxane hybrid coatings were prepared in two steps using sol-gel method. Acid catalyzed sol-gel method is applied to synthesize hybrid coatings [17]. Water:silane ratio, pH and catalyst concentration were optimized in this reaction depending on the desired end product. In first stage a sol of TEOS and GPTMS was prepared by sol-gel method. TEOS and GPTMS were reacted in 1:4 molar ratios in presence of 0.05M HCl. While preparing this sol the water ratio with respect to silanes was kept at 1:15 to acquire the desired sol for preparing hybrid coating. In second stage 1g of chitosan was dissolved in 1% of 100ml acetic acid. Then above prepared sol of GPTMS and TEOS was added dropwise in it and allowed it to stir for 72 hours at room temperature. Throughout the reaction the pH was maintained at 6.8. The reaction was carried out in a closed system as it is being a hydrolysis and condensation process. Chitosan-TEOS and chitosan-VTMS were also prepared by sol-gel method. In chitosan-TEOS system, chitosan solution was prepared in acetic acid in which TEOS was added in equimolar concentration. During this sol formation the water and pH were maintained at optimized concentration. Chitosan-VTMS sol was also prepared in the same way. During this sol preparation VTMS was added very slowly in chitosan solution and stirred vigorously as compared to TEOS and siloxane mixture as solubility of VTMS is less as compared to other two.

Sols prepared above are applied on glass microscopic slides of 17mm x 10mm. The glass slides were cleaned by soaking in 1M NaOH for 24 hours and then rinsed with copious amount of distilled water and ethanol. These treated

slides were then dried in ambient conditions and used for coating. These slides were coated by dip method. All coated slides were again stored at ambient conditions for at least one week. These coated slides and sols are then further analyzed.

Scheme 1 Mechanism of Chitosan-(GPTMS-TEOS) hybrid coating

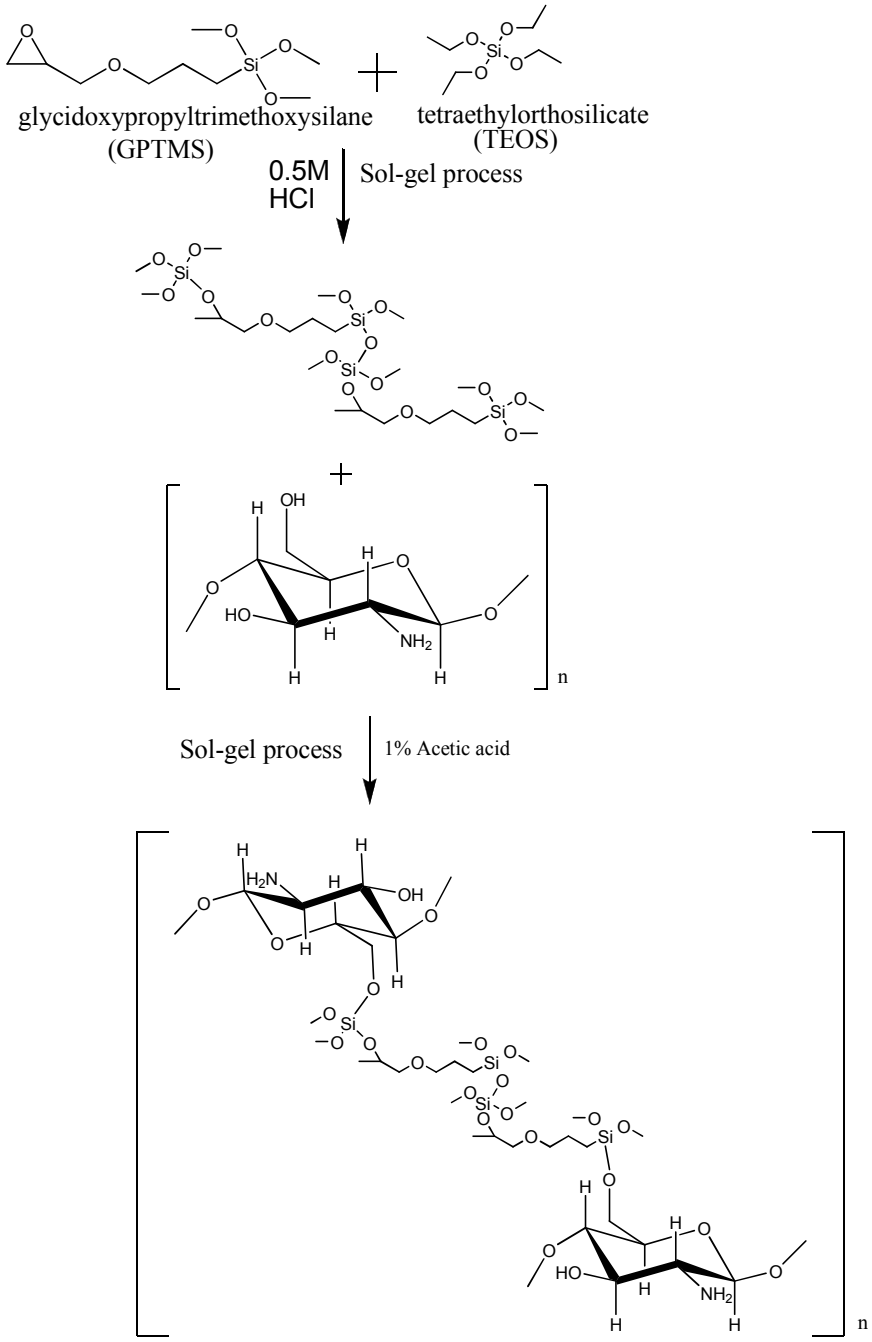

Chitosan-(GPTMS-TEOS) hybrid

Attenuated-Fourier transform infrared spectroscopy (AT-FTIR) was used to record IR of the sols on Shimadzu 8400 S. The evaluation was done at 256 scans with a resolution of 2 cm^{-1} in the range of 3400 and 600 cm^{-1}.

^{13}C Nuclear magnetic resonance (^{13}C-NMR) spectroscopy, ^{13}C solid state NMR spectra of hybrid coatings were recorded at 79.49 and 100.62 MHz, respectively, on a (9.4 T) Bruker Avance 500 spectrophotometer.

Scheme 2 Mechanism of Chitosan-TEOS hybrid coating

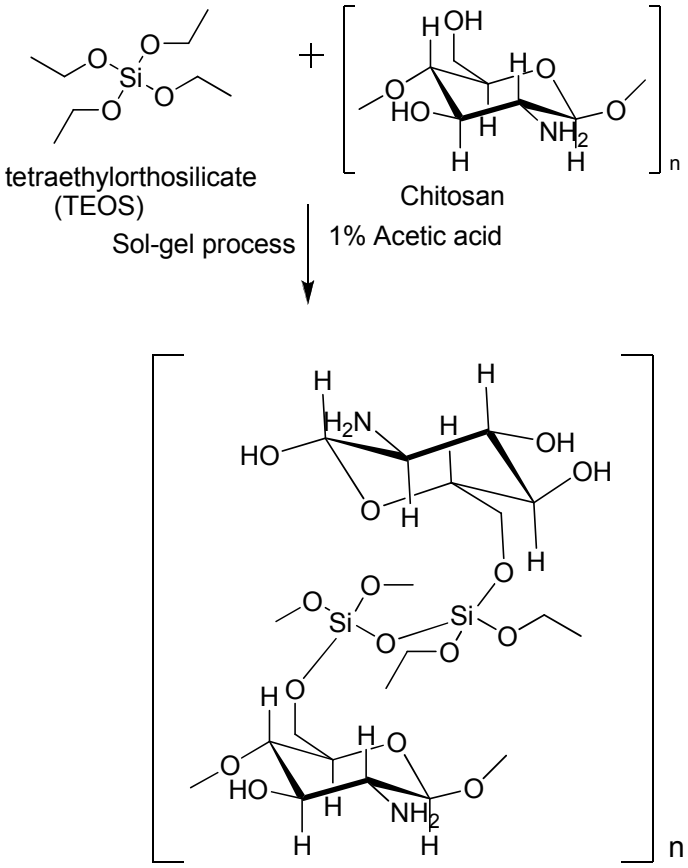

X-ray diffraction (XRD) patterns of hybrid coatings were recorded on Rigaku XRD-6000 diffractrometer for characterizing their crystalline pattern. Ni-filtered Cu Kα radiation was used as the X-ray source. The 2θ range was 10˚ to 40˚.

Thermal gravimetric analysis (TGA) of hybrid coatings were conducted with a Q-1500 D, TA instruments under N_2 atmosphere at a heating rate of 2˚C/min to characterize their thermal behavior. The range of scanning temperature was 50˚C to 500˚C.

Differential scanning calorimetry (DSC) measurements were obtained using TA instruments. Scans were obtained in the range of 20˚C to 500˚C with a heating rate of 10˚C/min.

Dynamic advancing and receding Contact angles were measured with distilled water on Kruss G10 contact angle meter at room temperature. These were recorded while water was added to and withdrawn from the drop, respectively, by a syringe pump. An average value of 3 drops of CA giving constant values was reported. Surface energy measurements of hybrid coatings were determined by first measuring the contact angle of water and hexadecane on hybrid surfaces and then calculating the surface energy by Fowkes' equation [52]:

$$\gamma_s = \gamma_1 (1+\cos\theta)^2/4$$

The surface morphology of the coatings were observed with a JEOL Model JSM 6380LA scanning electron microscope (Japan). A platinum coating was deposited on the samples to avoid charging the surface.

Coating samples were imaged with a "JPK Bio AFM, Nano Wizard II". The intermittent contact mode was applied for analyzing the samples. AFM imagination was performed at a set-point amplitute of 600mV. The drive amplitude was 0.05V and imaging was conducted just below the cantaliver resonant frequency of 298-300 kHz.

RESULTS AND DISCUSSION

2. 1. Synthesis

Sol gel is the proficient method of forming hybrid coatings. pH and water to silane ratio are some of the parameters which rule the reaction conditions responsible for the formation of the desired hybrid material [17]. Brinker [17] has reported that, at pH of 2-7 gel time decreases readily and metastable state of sol is obtained at pH 2-7. The pH of 6.8 is maintained throughout these reactions to acquire desired product. Brinker [17] has mentioned that the hydrolysis process in sol-gel method is performed between water:silane ratio of 1:25 depending upon the desired product. In the formation of these hybrid coatings the water ratio is maintained at molar ratio of 15 with respect to silane concentration considering maximum hydrolysis after keeping the reaction for 72 hours. The ethoxy and methoxy groups of TEOS and GPTMS respectively undergo hydrolysis and condensation converting these groups into hydroxyl groups leading to sol formation. This sol is then further added into chitosan solution where again hydrolysis and condensation takes place forming an organic-inorganic hybrid sol. The Si-OH group of sol of TEOS and GPTMS reacts with hydroxyl group at C-2 and C-6 position of chitosan as well as condensation of two Si-OH groups forms Si-O-Si network forming polymer. The reaction is depicted in (**Scheme 1)** of Chitosan-Mix hybrid. In chitosan-TEOS sol, the ethoxy group of TEOS undergoes hydrolysis giving hydroxyl group which then further reacts with the hydroxyl group of chitosan which is shown in (**Scheme 2).** The chitosan-VTMS hybrid coating is formed by hydrolysis of methoxy group of VTMS which then further reacts with chitosan forming siloxane – polymer network as exhibited in (**Scheme 3).**

Scheme 3 Mechanism of Chitosan-VTMS hybrid coating

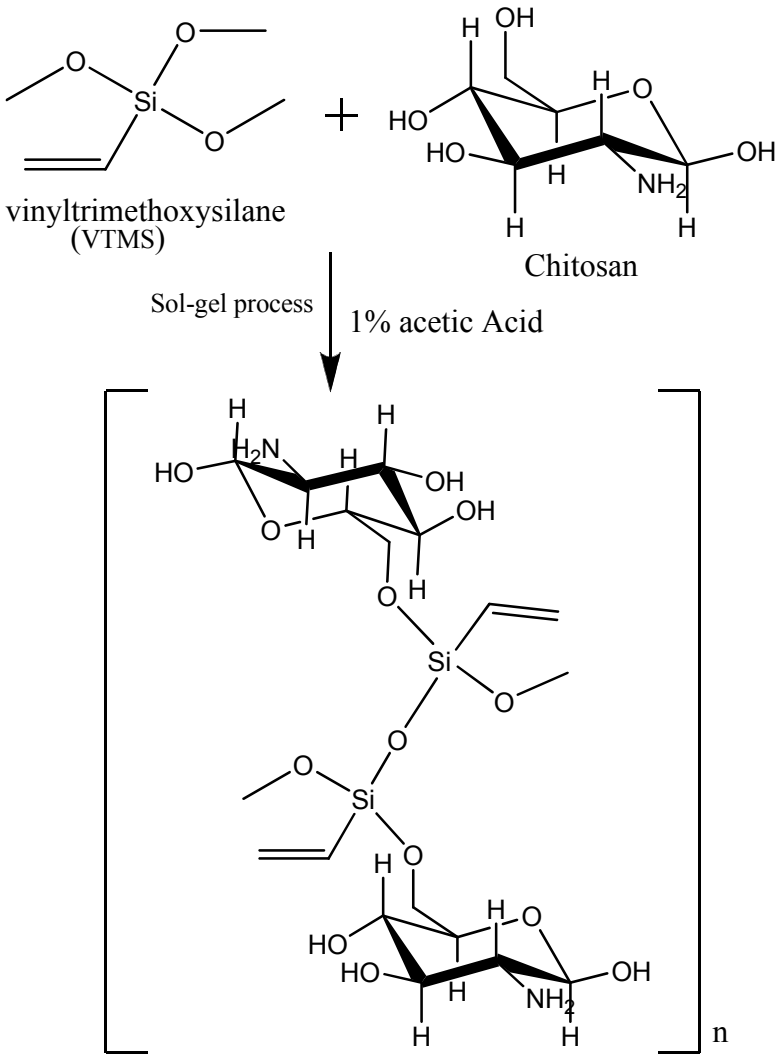

Chitosan-VTMS hybrid

2.2. Characterisation

The AT-FTIR graph of hybrid materials is illustrated in **Figure. 1**. The hydroxyl stretching of chitosan occurs at 3353 cm^{-1} which overlaps with amine band. –CH stretching appears at 2924cm^{-1}. –C=O appears at 1630-1670 cm^{-1}. –NH (hydrogen bonded) gives a peak at 1557 cm^{-1}. Peak appearing at 1023cm^{-1} is attributed to –C-O stretching. These results indicate presence of hydrogen bonding within the molecular chain in pristine chitosan. In all the three hybrid coatings formed by incorporation of silica in situ, all the above mentioned chitosan bands remain unchanged in hybrid coatings. The inorganic phase gives IR bands in the following regions: 1137-1000, 950-900 and 800-700 cm^{-1} assigned respectively to Si-O-Si (stretch), Si-OH (stretch) and Si-O-Si. The broad peak appearing at 3353cm^{-1} in chitosan becomes narrow in all the hybrid coatings due to incorporation of silica. The intensity of the interaction of hydrogen bonding between Si-O on silica and functional groups on chitosan decreases in the –N-H region in chitosan-silica hybrid coatings. Such a decrease is observed in intensity of the peak at 1557cm^{-1} which is attributed to hydrogen bonded amine group with Si-O on silica. The band of chitosan- (TEOS and GPTMS) hybrid coating appearing at 2946cm^{-1} is due to presence of $–CH_2$ of GPTMS of hybrid. Intensity of the band appearing at 1100-1000 increases mostly due to overlapping of the Si-O-Si and –C-O-C- of glycosidic linkage. The overlapping of these bands is reported previously in literature [22]. The IR graph of chitosan-TEOS hybrid coating shows all the peaks of pristine chitosan as well as peaks of inorganic moiety. In IR graph of chitosan-VTMS hybrid coating all the above mentioned peaks for chitosan as well as inorganic peaks are present besides it gives a characteristic peak of vinyl group at 1639 cm^{-1} confirming the presence of vinyl group in hybrid. As mentioned earlier the intensity of hydrogen bonding decreases in the –NH region in chitosan-silica hybrid is seen even in the hybrid coatings which are formed here.

Figure 1. FTIR spectra of chitosan-siloxane hybrids: a) Chitosan-(GPTMS-TEOS); b) Chitosan-TEOS; c) Chitosan-VTMS hybrid coatings.

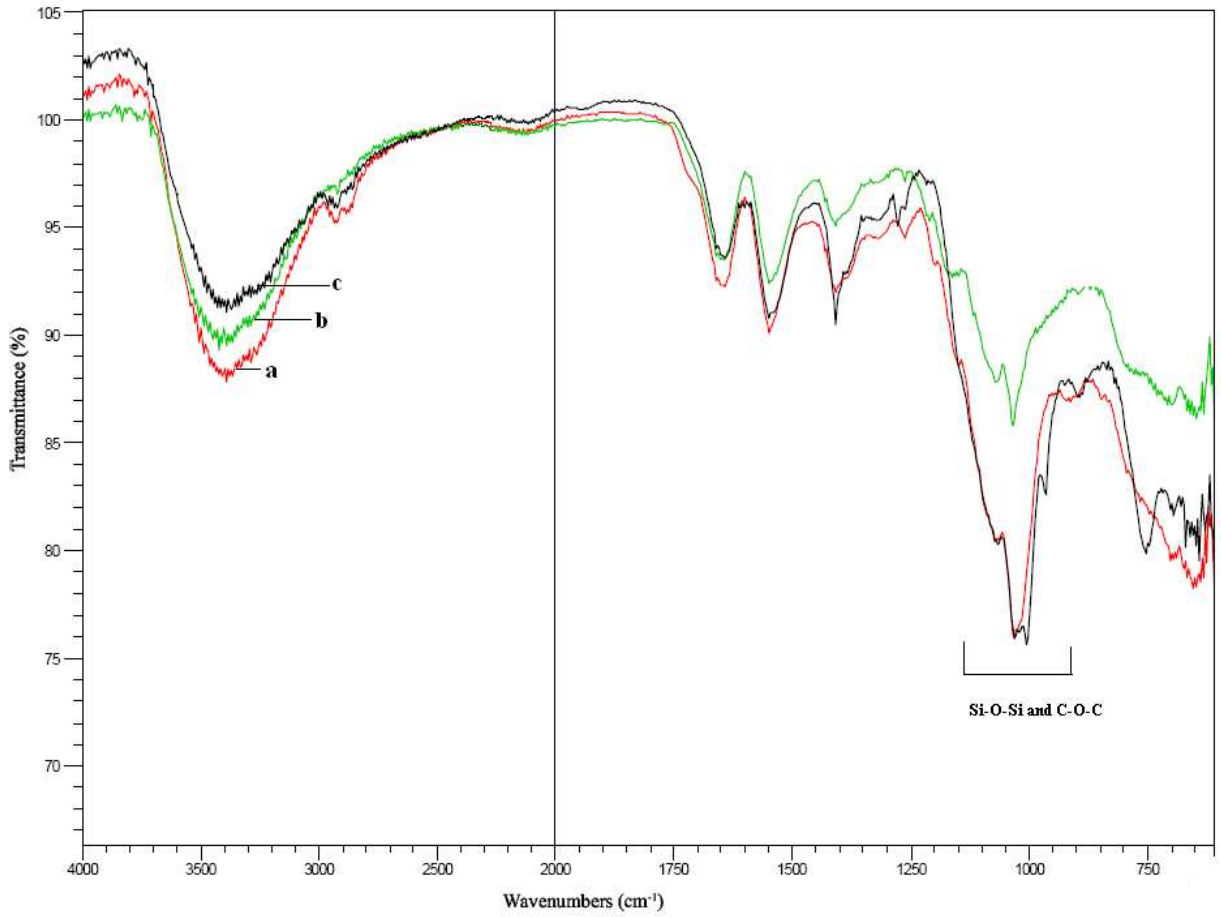

^{13}C-NMR spectra of chitosan-siloxane hybrid coatings are represented in **Figure. 2.** where appearance of signals at 61.99 and 66.47 confirms the formation of the bridge between siloxane network to the polymer. Shift at 25.54 confirms primary amine of chitosan. Chemical shift at 11.93 is assigned for $-CH_3$ of GPTMS. Band appearing at 77.22 confirms -C-O-C- linkage of chitosan chain adjacent to $–CH_2OH$, whereas the band appearing at 105.10 is due to -C-O-C- linkage adjacent to oxygen present in the glycosidic ring. Chitosan-TEOS also shows all the chemical shifts appearing in chitosan-(GPTMS-TEOS) but they are slightly shifted to upfield as the electronegativity is less in

Chitosan-TEOS as compared to chitosan-(GPTMS-TEOS). In Chitosan-VTMS all the chemical shifts are similar to chitosan-(GPTMS-TEOS), in addition to it peaks at 138 and 132 are ascribed to vinyl group present in the hybrid.

Figure 2. ^{13}C- NMR of chitosan-siloxane hybrid coatings: a) Chitosan-(GPTMS-TEOS); b) Chitosan-TEOS; c) Chitosan-VTMS

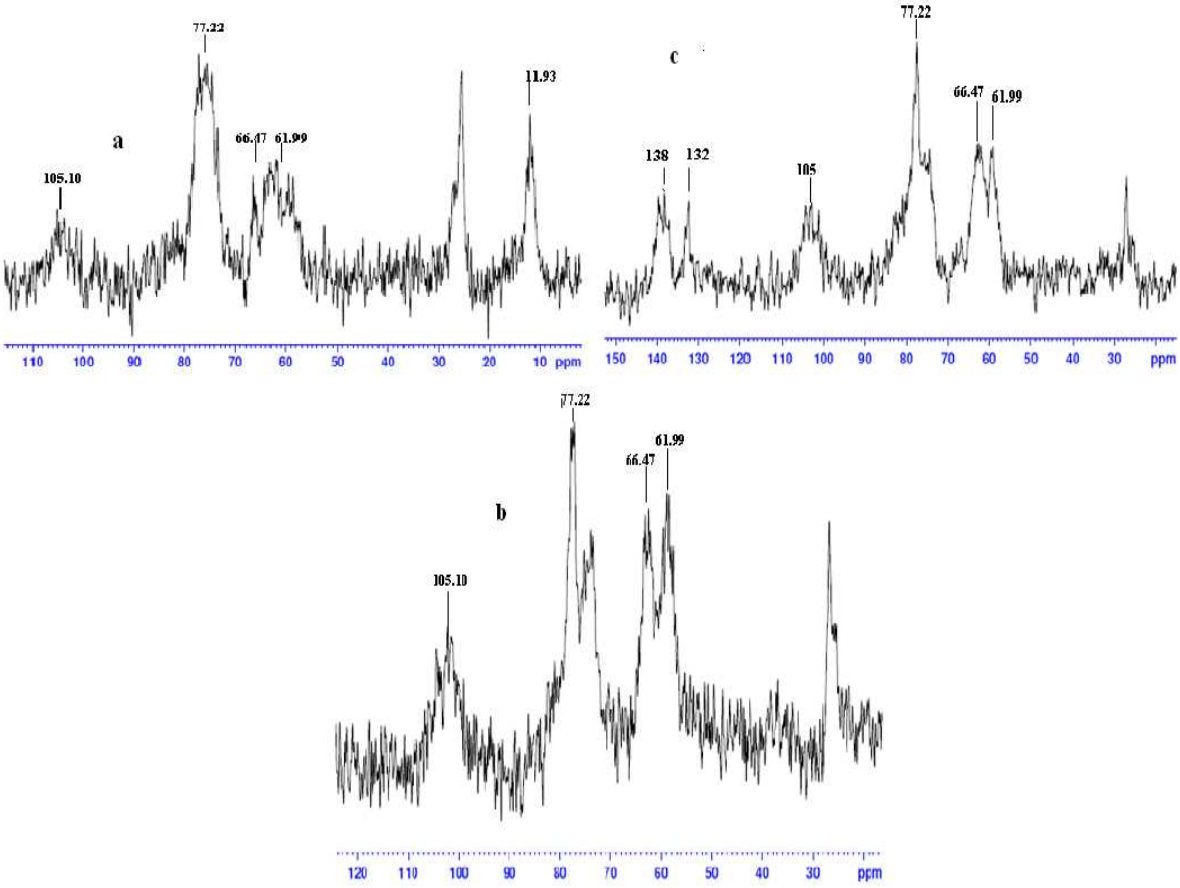

To investigate the structure of hybrid coatings, the XRD measurement was carried out with result showing in **Figure. 3**. The peak observed at 20.02° is associated with the crystalline structure of chitosan. The characteristic diffraction peaks of silica are generally observed at 2θ= 17.8°, 19.1° and 20.6°. In every chitosan/silica hybrid coatings only one peak at 2θ=20.4° is observed. This is consequently due to disturbance of crystalline form. This disturbance occurs due to interaction between chitosan and silica in hybrid coatings, due to which the region of 2θ from 15° to 20° becomes broad. This broadness of peak is more in chitosan-(GPTMS-TEOS) than chitosan-TEOS hybrid coatings as the amount of silica in it is more due to which silica aggregation disturbs the crystallinity. The shoulder appearing at 10° in pure chitosan is ascribed to other form of ordering within the chitosan chains, with a characteristic distance of 8.5±0.3A°. In hybrid coatings the peak at 8.5±0.3A° is not seen but two broad and weak humps are present at 8.5-9.0 and 12.0-12.5. The peak emerging at low angles, 6° in hybrid materials are assigned to interparticle scattering interference and indicates highly non-periodic fluctuation of the electronic density in these hybrid materials. This peak is characteristic of aggregation of silica at high silylating agent [47]. The crystallinity of hybrid coatings decreases as compared to chitosan on addition of silylating agent. This attributes to breaking of intrinsic hydrogen bonding between hydroxyl and amine groups of chitosan chains and formation of hybrid by interchain linkages between polysiloxane and chitosan chains [47]. This phenomenon is observed in every chitosan-silica hybrid coatings which are formed. In chitosan-VTMS hybrid coating the peaks appearing at 6° and 20.4° are evident than chitosan-(GPTMS-TEOS) and chitosan-TEOS hybrid coatings. This phenomenon in chitosan-VTMS hybrid coating is attributed to formation of silica aggregation and steric hindrance of vinyl group.

Figure 3. XRD curves of chitosan and chitosan-siloxane hybrids: a) Chitosan-(GPTMS-TEOS); b) Chitosan-TEOS; c) Chitosan-VTMS hybrid coatings.

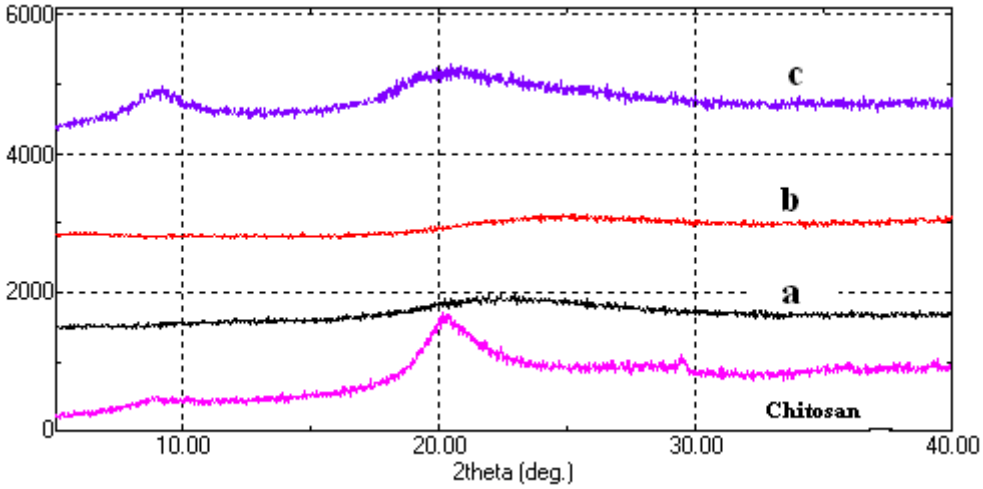

The thermal stability of chitosan-siloxane hybrid coatings is evaluated by thermogravimetric analysis. The thermograms are shown in **Figure. 4**. The first weight loss at around 100ºC is attributed to loss of water molecules present in the hybrid coating. The second weight loss appearing at around 280ºC-300ºC indicates decomposition of hybrid coatings and the third weight loss is observed near 380ºC. Such changes clearly indicate hybridization between organic and inorganic parts. In hybrid coatings the polymeric matrix is forming due to covalent linkage between chitosan and silylating agents and the Si-O-Si linkages. AT-FTIR supports formation of this polymer linkage. The weight loss appearing at around 280ºC is due to unstable parts of polymeric matrix whereas the third weight loss is occurring due to complete decomposition of the backbone of the polymeric matrix. It is considered that the improvement in thermal stability which occurs in hybrid coatings is due to different silanes. As it is evident from the thermograms of hybrid coatings, chitosan-(GPTMS-TEOS) is more thermally stable than chitosan-TEOS and chitosan-VTMS. The chitosan-(GPTMS-TEOS) hybrid has mixture of silylating agents therefore it is more stable, as inorganic portion is increasing in this hybrid. In literature it is mentioned that thermal stability of chitosan increases on high content of silylating agent [47]. Thermal stability of chitosan-TEOS hybrid is more as compared to chitosan-VTMS because for SiO_2 to take shape is hard due to steric hindrance of vinyl group of chitosan-VTMS. It can be seen that chitosan-silica hybrid coatings has exhibited better thermal stability than the pristine chitosan. It is reported that silica formed serves as a protective material which impedes thermal degradation of chitosan resulting in retardation on thermal degradation and enhancement on char formation [48]. Thus, the same trend is observed in temperature of weight loss of hybrid coatings which shifts towards higher temperature area and even the char yield of hybrid coatings is more than the pristine chitosan as can be seen from (Table 1), indicating higher thermal stability of hybrid coatings which is due to formation of stable silica.

Table 1 Thermal properties of chitosan-siloxane hybrids: a) Chitosan-(GPTMS-TEOS); b) Chitosan-TEOS; c) Chitosan-VTMS hybrid coatings

Material	Thermal properties		Char Yield
	T^a(°C)	T^b(°C)	(%)
Chitosan	245	315	36
Chitosan-(GPTMS-TEOS)	203	272	40
Chitosan-TEOS	158	360	37
Chitosan-VTMS	218	393	38

T^a Temperature at 10% loss
T^b Temperature at maximum weight loss

The glass transition temperatures measured by DSC for chitosan-silica hybrid coatings are displayed in **Figure. 5**. The glass transition temperature of hybrid coatings are determined according to ASTM standard E1356 standard test method for assignment of glass transition temperatures by differential scanning calorimetry. This gives the midpoint temperature between extrapolated onset and endset of endotherm. Glass transition temperature increases on incorporation of silica in chitosan as it is reported in cases of silica containing polyimides [49]. Tg of pristine chitosan is at around 58°C (Figure not shown for brevity). It is being observed that the glass transition temperature (Tg) of hybrid coatings is shifted to higher values than the pristine chitosan. In chitosan-(GPTMS-TEOS) Tg is observed at 75°C, this behavior is related to the modification of chitosan with siloxane. The restricted segmental mobility in chitosan-(GPTMS-TEOS) hybrid is due to silica network formation in chitosan as this phenomenon is supported by AT-FTIR. Hybrid of chitosan-VTMS illustrates Tg at 68°C. It is observed that the glass transition

temperature of chitosan-VTMS is higher than pristine chitosan indicating limitations of segmental mobility induced by silica network as well as double bond of VTMS. Glass transition temperature of chitosan-TEOS is 70°C, which is less than chitosan-(GPTMS-TEOS) due to absence of GPTMS in chitosan-TEOS.

Figure 4. TGA thermograms of chitosan-siloxane hybrids: a) Chitosan-(GPTMS-TEOS); b) Chitosan-TEOS; c) Chitosan-VTMS hybrid coatings.

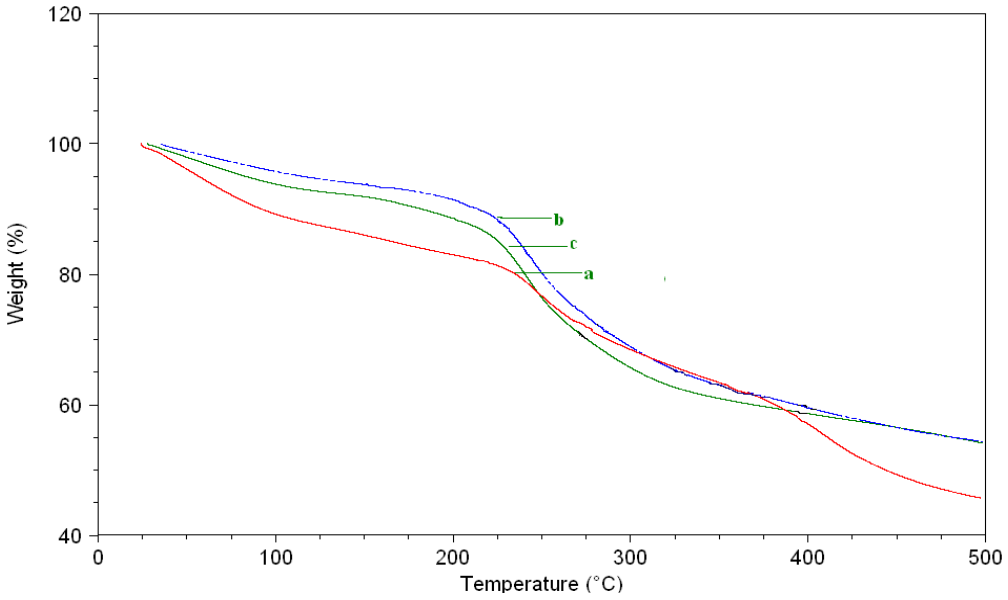

Figure 5. DSC curves of chitosan-siloxane hybrids: a) Chitosan-(GPTMS-TEOS); b) Chitosan-TEOS; c) Chitosan-VTMS hybrid coatings.

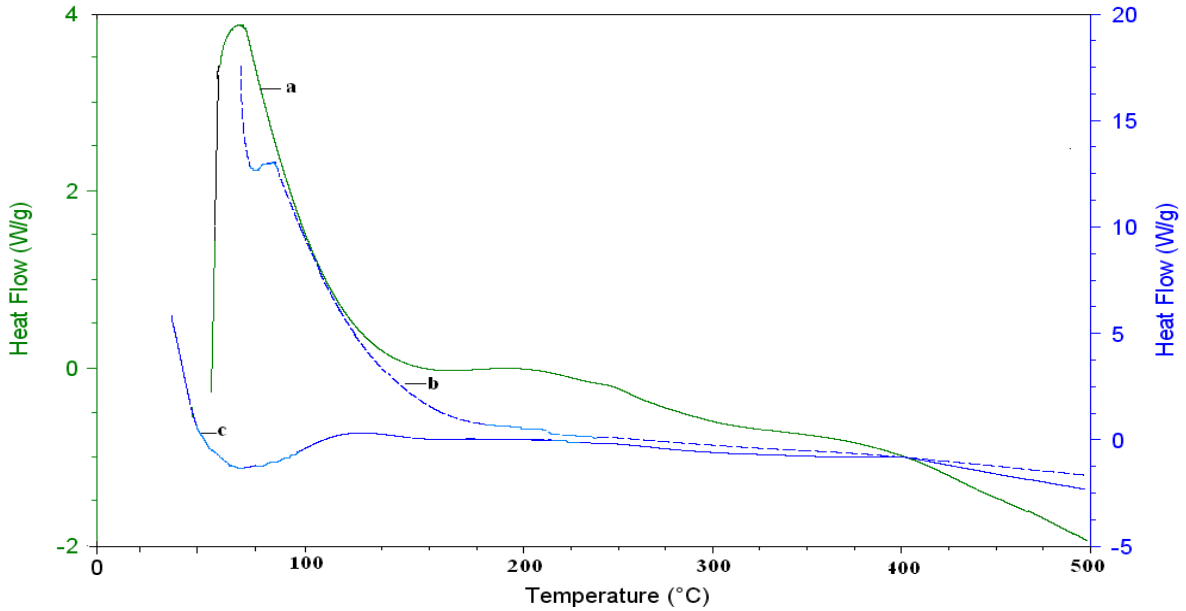

The surfaces of hybrid coatings are characterized by contact angle and it is summarized in table 2. The contact angles are important to ascertain the hydrophilicity or hydrophobicity of these hybrid coatings. The effect of different silanes on hydrophobicity of chitosan and silica hybrid coatings is discussed. In chitosan-(GPTMS-TEOS) hybrid coating where chitosan is modified using TEOS and GPTMS, the contact angle is measured at 73º. The contact angle of chitosan-TEOS hybrid coating is observed at 67º and the contact angle of chitosan-VTMS hybrid coating is measured at 75º. Silanes provide hydrophobicity or hydrophilicity by changing the interaction of boundary layer of solids with water [50]. Therefore chitosan has been modified with different silanes considering that this modification will provide different hydrophobicity or hydrophilicity to hbrid coatings. It has been observed that chitosan-VTMS hybrid coating shows more hydrophobicity than the other two hybrid coatings. This indicates more

hydrophobic nature developed due to VTMS. Silica nanoparticles on modification by vinyl groups develop superhydrophobic silica nanoparticles. The modification results in surface reorientation in which the hydroxyl groups on the surface are substituted by vinyl groups and the hydroxyl groups present inside remains unchanged [51]. Chitosan-TEOS system is more hydrophilic as compared to other two hybrid coatings. This hydrophilicity appears in this coating due to more of hydroxyl groups as well as more of hydrogen bonding sites available for bonding with water in it. The surface energies of hybrid coatings have been evaluated using mean contact angles of hybrid coatings (Table2). The surface energy of chitosan-VTMS hybrid has very low as compared to other two hybrid coatings, which would confirm the presence of vinyl groups on the surface creating hydrophobicity. The surface energy of chitosan-(GPTMS-TEOS) is less as compared to chitosan-TEOS resulting due to presence of alkyl groups of GPTMS which provides hydrophobicity. The surface energy illustrates the roll-on effect of water on these hybrid coatings whereas in case of hexane the roll-on effect decreases explaining that the hybrid has more affinity towards hexane than water.

Figure 6. SEM images of chitosan-siloxane hybrids: a) Chitosan-(GPTMS-TEOS); b) Chitosan-TEOS; c) Chitosan-VTMS hybrid coatings.

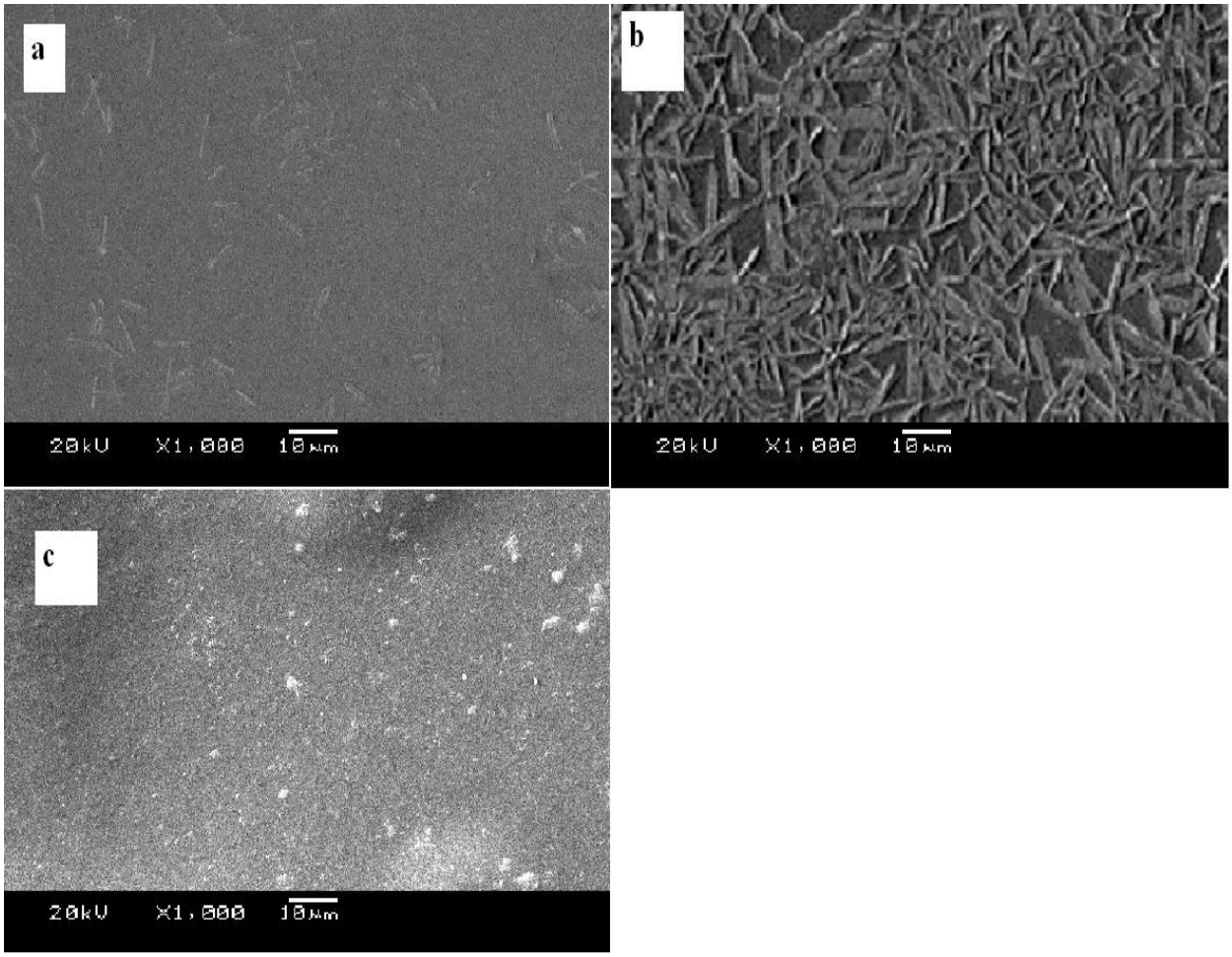

Table 2 Contact Angles and Surface energies of chitosan-siloxane hybrids: a) Chitosan-(GPTMS-TEOS); b) Chitosan-TEOS; c) Chitosan-VTMS hybrid coatings

Materials	Contact angle θ°				Surface energy (S.E) mN/m	
	Water		Hexadecane		Water	Hexadecane
	Advθ°	Recθ°	Advθ°	Recθ°		
Chitosan-(GPTMS-TEOS)	73	20	18	8	30.39	26.14
Chitosan-TEOS	67	29	21	6	35.20	25.67
Chitosan-VTMS	75	18	12	9	28.84	13.28

$(S.E)^b$: $\gamma\ (1+ \cos\theta a)^2/4$

Where, γ is the surface tension of wetting liquid.
Γ of water = 72.8 mN/m
Γ of hexadecane = 27.47mN/m

The surface morphology of the hybrid coatings are revealed by scanning electron microscopy. Fig. 6a and b shows needle like structures. Therefore, it is evident that these hybrid materials which are made of chitosan and GPTMS and TEOS in them have an acerose surface with interspaces for less inorganic SiO_2. The dentritic structure is more in chitosan-TEOS as compared to chitosan-(GPTMS-TEOS) it can be considered that TEOS is forming this structure. Chitosan-VTMS exhibits a firm and imporous surface. The homogenous distribution of silica in chitosan hybrid is evident from the bright spots representing the silicon element in Fig. 6c.

AFM technique is used to evaluate the surface texture of the hybrid coatings. Roughness profiles of the hybrid coatings are shown in **Fig.7**. The surface roughness is measured as average roughness which is calculated as the distance between the deepest and highest point on the given surface of 2.5µm x 2.5µm. The roughness parameters of the hybrid coatings are analyzed to show the average roughness of these hybrid coatings. It is being observed that the surface roughness of chitosan-(GPTMS-TEOS) is 31nm, chitosan-TEOS is 24nm and chitosan-VTMS is 20nm. The surface roughness increases on increase in silylating agent. The roughness of chitosan-(GPTMS-TEOS) having two silylating agents exhibits more surface roughness than the other two hybrid coatings. The AFM graph of all the hybrid coatings shows wavy open texture as can be seen from Fig.6 indicates smoothness of the hybrid coatings. This is attributed to even distribution of chitosan and silica in hybrid coatings.

Figure 7. AFM images of chitosan-siloxane hybrids: a) Chitosan-(GPTMS-TEOS); b) Chitosan-TEOS; c) Chitosan-VTMS hybrid coatings.

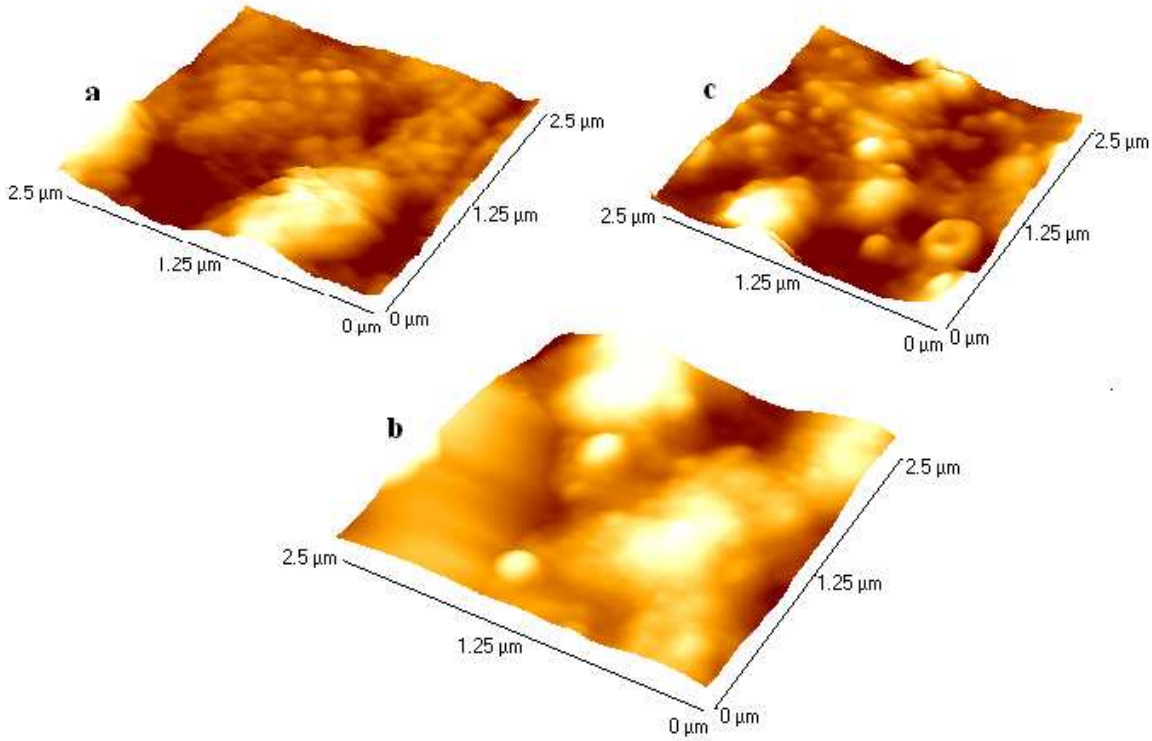

CONCLUSION

The present work deals with the structural, physical and thermal investigation of chitosan-silica hybrid coatings constructed by sol-gel process from chitosan and different silane precursors. Modification of chitosan with different silanes was successful by the sol-gel method. AT-FTIR and ^{13}C-NMR analysis exhibits formation of hybrid coatings from chitosan and different silanes. These analyses confirm the attachment of siloxane moieties to chitosan and formation of siloxane-polymer network. These analysis also reveals the presence of different silanes in the respective hybrid coatings. The thermal stability of hybrid coatings is achieved due to silanes. When two silane precursors were used thermal stability has increased appreciably. The glass-transition phenomenon observed by

DSC in these hybrid materials correspond to the results of TGA. The hybrid coatings show good wettability. The surface energy results explain the roll-on effect of hybrid coatings. SEM results indicate the presence of different silanes used in hybrid coatings due to distinguished morphological structures showed by every silane. The surface morphology of hybrid coatings shows homogenous distribution of silane in chitosan polymer. The surface roughness of these hybrid coatings is increasing on increasing silylating agent is obtained from AFM analysis. These hybrid coatings show the potential of being used as bioactive coating materials for marine application. Further investigations of coatings are in progress in order to use these hybrid coatings especially in antifouling coatings.

Acknowledgements
The authors acknowledge UGC-SAP for financial support. The authors also like to thanks TIFR for assistance in NMR and Department of Dyestuff Technology, Institute of Chemical Technology for assistance in TGA analysis.

REFERENCES

[1] Silva, S.S.; Ferreira, R.A.S.; Fu, L.; Carlos, L.D.; Mano, J.F.; Reis, R.L.; Rocha, J. *J. Mater. Chem*. **2005**, 15, 3952-3961.
[2] Shin, J. H.; Weinman, S. W.; Schoenfisch, M. H. *Anal. Chem.*, **2005**,77, 3494-3501.
[3] Li, F.; Du, P.; Chen, W.; Zhang, S. S. *Anal. Chim. Acta*. **2007**, 585, 211-218.
[4] Li, F.; Li, X. M.; Zhang, S. S. *J. Chromatogr. A.* **2006**, 1129, 223-230.
[5] Romero, P.G.; Sanchez, C. (eds.), Functional hybrid materials. Wiley- VCH, Weinheim, **2004**.
[6] Dave, B.C.; Soyez, H.; Miller, J.M.; Dunn, B.; Valentine, J.S.; Zink, J.I. *Chem. Mater*. **1995**, 7, 1431-1434.
[7] Jiang, Y.; Zhang, L.; Yang, D.; Li, L.; Zhang, Y.; Li, J.; Jiang, Z. *Ind. Eng. Chem. Res*. **2005**, 47, 2495-2501.
[8] Jiang, Y.; Yang, D.; Zhang, L.; Sun, Q.; Sun, X.; Li, J.; Jiang, Z. *Adv. Funct. Mater*. **2009**, 19, 150-156.
[9] Gill, I.; Ballesteros, A. Bioencapsulation within synthetic polymers (Part 1): sol–gel encapsulated biological. Tibtech, july **2000**, 18, 228-296.
[10] Singh, A. K.; Singh, P.; Mishra S.; Shahi, V. K. *J. Mater. Chem*. **2012**, 22, 1834-1844.
[11] Gunari, N.; Brewer, L. H.; Bennett, S.M.; Sokolova, A.; Kraut, N.D.; Finlay, J. A.; Meyer, A.E.; Walker, G. C.; Wendt, D. E.; Callow, M. E.; Callow, J. A.; Bright, F. V.; Detty, M. R. *Biofouling*. **2011**, 27, 2, 137–149.
[12] Coradin, T.; Bah, S.; Livage, J. *Colloids Surf. B: Biointerfaces*. **2004**, 35, 53-58.
[13] Ren, L.; Tsuru, K.; Hayakawa, S.; Osaka, A. *Biomaterials*. **2002**, 23, 47654773.
[14] Brasack, I.; Bottcher, H.; Hempel, U. *J. Sol–Gel Sci. Technol*. **2000**, 19, 479-482.
[15] Ren, L.; Tsuru, K.; Hayakawa, S.; Osaka, A. *J. Sol–Gel Sci. Technol*. **2001**, 21, 115-121.
[16] Ren, L.; Tsuru, K.; Hayakawa, S.; Osaka, A. *J. Non-Cryst. Solids*. **2001**, 285, 116-122.
[17] Brinker, C.J.; Scherer, G.W. Sol–Gel Science: The Physics and Chemistry of Sol–Gel Processing, Academic Press, NY, USA, **1990**.
[18] Chen, Q.; Miyaji, F.; Kokubo, T.; Nakamura, T. *Biomaterials*. **1999**, 20, 1127-1132.
[19] Sequeira, S.; Evtuguin, D.V.; Portugal, I.; Esculcas, A.P. *Mater. Sci. Eng*. **2007**, 27, 172-179.
[20] Cao, W.; Easley, C.J.; Ferrance, J.P.; Landers, J.P. *Anal. Chem*. **2006**, 78, 7222-7228.
[21] Molvinger, K.; Quignard, F.; Brunel, D.; Boissiere, M.; Devoisselle, J.M. *Chem. Mater*. **2004**, 16, 3367-3372.
[22] Yeh, J.T.; Chen, C.L.; Huang, K.S. *Mater. Lett*. **2007**, 61, 1292-1295.
[23] Kadib, A.E.; Molvinger, K.; Guimon, C.; Quignard, F.; Brunel, D. *Chem. Mater*. **2008**, 20, 2198-2204.
[24] Marques, P.A.A.P.; Trindade, T.; Neto, C.P. *Compos. Sci. Technol*. **2006**, 66, 1038-1044.
[25] Watzke, H.J.; Dieschbourg, C. *Adv. Colloid Interface Sci*. **1994**,50, 1-14.
[26] Schuleit, M.; Luisi, P.L. *Biotechnol. Bioeng*. **2001**, 72, 249-253.
[27] Liu, D.M.; Chen, I.W. *Acta Mater*. **1999**, 47, 4535-4544.
[28] Yuan, G.L.; Yin, M.Y.; Jiang, T.T.; Huang, M.Y.; Jiang, Y.Y. *J. Mol. Catal. A: Chem.* **2000**, 159, 45-50.
[29] Göltner, C.G.; Berton, B.; Krämer, E.; Antonietti, M. *Adv. Mater*. **1999**, 11, 395-398.
[30] Kurita, K. *Polymer Degradation and Stability*. **1998**, 59, 2, 117-120.
[31] Yadav, A.V.; Bhise, S. B. *Current Science*. **2004**, 87, 9, 1176-1178.
[32] Raafat, D.; Bargen, K. V.; Haas, A.; Sahl, H. G. *Appl. Environ. Microb*. **2008**, 74, 12, 3764-3773.
[33] Liu, X. F.; Guan, Y. L.; Yang, D. Z.; Li, Z.; Yao, K. D. *J. Appl. Polym. Sci*. **2001**, 79, 7, 1324-1335.
[34] Entsar, I. R.; Moham, E. T. B.; Christian, V. S.; Gay, S.; Walter, S. *Biomacromolecule*. **2003**, 4, 6, 1457-1465.
[35] Kalyan, S.; Sharma, P. K.; Garg, V. K.; Kumar, N.; Varshney, J. *Der Pharmacia Sinica*. **2010**, 1 (3), 195-210.
[36] Patel, P. N.; Patel, L. J.; Patel, J. K. *Der Pharmacia Sinica*. **2011**, 2 (4):17-25.
[37] Garg, A.; Visht, S.; Sharma, P. K.; Kumar, N. *Der Pharmacia Sinica* **2011**, 2 (2): 17-26.
[38] No, H. K.; Meyers, S. P.; Prinyawiwatkul, W.; Xu, Z. *Journal of food science*.**2007**, 72, 5, R87-R100.
[39] Ramachandran, T.; Rajendrakumar, K.; Rajendran, R. *India Journal Textile*. **2004**, 84, 2, 42-47.
[40] Aly, S.; Jeon, B. D.; Park, Y. H. *Journal of Applied Polymer Science*. **1997,** 65, 10, 1939-1946.
[41] Shih, Y.; Chen, C. W.; Huang, K. S. *Journal of Applied Polymer Science*. **2004,** 91, 6, 3991-3998.
[42] Wada, T.; Uragami, T.; Matoba, Y. *Journal of Coatings Technology and Research*. **2005**, 2, 7, 577-592.

[43] El-Sayed, G. O.; Mohammed T. Y.; El-Sayed, O. E. *Advances in Applied Science Research*, **2011**, 2 (4), 283-290.
[44] Serag, H.; Edrees, G. *European Journal of Experimental Biology*. **2011**, 1 (4), 87-92.
[45] Al-Sagheer, F.; Muslim, S. *Journal of Nanomaterials*. **2010**, 1-7.
[46] Xu, X.; Dong, P.; Feng, Y.; Li, F.; Yu, H. *Anal. Methods*. **2010**, 2, 546–551.
[47] Xi, F.; Wu, J.; Lin, X. *Journal of Chromatography* A. **2006**, 1125, 38–51.
[48] Liu, Y. L.; Su, Y. H.; Lai, J. Y. *Polymer*. **2004**, 45, 6831–6837.
[49] Nandi, M.; Conklin, J. A.; Salviati, L. Jr.; Sen, A.; *Chem. Mater*. **1990,** 2, 6, 772-776.
[50] Arkles, B. Hydrophobicity, hydrophilicity and silane surface modification. Gelest Inc. **2006,** 1-76. www.gelest.com.
[51] Xue, L.; Li, J.; Fu, J.; Han, Y. *Physicochem. Eng. Aspects*. **2009**, 338, 15–19.
[52] Fowkes, F. M. *Ind. Eng. Chem*. **1964,** 56(12), 40-52.